

RESEARCH PAPER

## Microwave Aided Synthesis of Silver and Gold Nanoparticles and their Antioxidant, Antimicrobial and Catalytic Potentials

Sijo Francis<sup>1</sup>, Ebey Koshy<sup>1</sup> and Beena Mathew<sup>2\*</sup>

<sup>1</sup> Department of Chemistry, St. Joseph's College, Moolamattom, Idukki, Kerala, India

<sup>2</sup> School of Chemical Sciences, Mahatma Gandhi University, Kottayam, Kerala, India

### ARTICLE INFO

#### Article History:

Received 10 November 2017

Accepted 22 December 2017

Published 01 January 2018

#### Keywords:

DPPH

Dye degradation

Green synthesis

*Jatropha curcas*

Metal nanoparticles

Well diffusion

### ABSTRACT

Here we reported the extremely simple one-pot synthesis of silver and gold nanoparticles in a rapid manner. Aqueous leaf extract of the most admired energy plant *Jatropha curcas* is used as reducing agent here. An alternate and safe energy source, house-hold microwave oven constituted the reaction chamber. Silver and gold nanoparticles were characterized by UV-visible, FT-IR, Powder XRD techniques. Surface plasmon resonance peaks corresponding to silver and gold nanoparticles were 428 nm and 543 nm respectively. The XRD patterns were indexed to reflections originated from (111), (200), (220) and (311) faces of FCC nanosilver and nanogold. Microscopic analysis revealed spherical geometry of silver nanoparticles with an average diameter  $20.42 \pm 12.2$  nm. Gold nanometals exhibited uneven shapes with average size  $17.12 \pm 2.9$  nm. In-vitro antioxidant potential assessment by DPPH model gave  $IC_{50}$  values  $19.37 \pm 0.63$  and  $16.59 \pm 0.29$   $\mu\text{g}/\text{mL}$  for silver and gold nanoparticles. The nanometals showed excellent bactericidal activity in agar well diffusion towards microorganisms namely *Bacillus cereus*, *Staphylococcus aureus*, *Escherichia coli*, *Pseudomonas aeruginosa*, *Aspergillus nidulans* and *Aspergillus flavus*. Degradation of methylene blue and rhodamine B by  $\text{NaBH}_4$  happened within 10 minutes in the catalytic presence of silver/gold nanoparticles offered a new means for purification of industrial dye effluents. Hydrogenation of 4-nitrophenol in presence of the prepared nanoparticles validated their catalytic utility. The reaction followed pseudo-first order kinetics with respect to reactant concentration.

### How to cite this article

Francis S, Koshy E, Mathew B. Microwave Aided Synthesis of Silver and Gold Nanoparticles and their Antioxidant, Antimicrobial and Catalytic Potentials. J Nanostruct, 2018; 8(1): 55-66. DOI: 10.22052/JNS.2018.01.007

### INTRODUCTION

Environmental concerns and green chemistry perspectives were highly satisfied in nanoparticles synthesis using natural resources [1]. Green synthetic strategies of nanometals mainly concentrated on green solvents, reducing agents and capping agents [2]. The most eco-friendly solvent water reduced pollution and price. Various pathways of nanoparticles synthesis included chemical, physical, electrochemical and biological reduction methods. Bacterial/ fungal preparation

\* Corresponding Author Email: [beenams@cmu.ac.in](mailto:beenams@cmu.ac.in)

procedures assured purity of the product with reduced toxicity of byproducts and wastes [3]. But it required time and tedious procedures of preparation. Plant extracts offered viable alternatives which can be served as both reducing and stabilizing agents [4]. Microwave irradiation technique (MIT) was an effective and effortless method for the preparation of metal nanoparticles [5,6]. Size and shape of nanoparticles were tuned by altering the amount of reaction ingredients and conditions. Plant reduced noble nanometals have



This work is licensed under the Creative Commons Attribution 4.0 International License.

To view a copy of this license, visit <http://creativecommons.org/licenses/by/4.0/>.

medical utility because of their biocompatibility [7].

*Jatropha curcas* (*J. curcas*), one of the most explored plants belonged to family of Euphorbiaceae and has high industrial importance. Being largely used in biomass plantations and soil manure purposes, the waste land plant served humanity a lot [8]. Literature showed that the latex and seed extracts of *J. curcas* were used as reducing and capping agents in silver nanoparticles' synthesis [9,10]. Carbonyl, hydroxyl and amino functional groups were responsible for the reduction and cyclic peptides and the enzyme curcain performed the capping action. Biogenic gold nanoparticles has been prepared from aqueous shell and seed meal extracts of *J. curcas* [11]. Recently published article explained the room temperature synthesis of silver nanoparticles using this plant leaves and exhibited growth inhibition against food borne microorganisms [12].

In the present work aqueous leaf extract of *Jatropha curcas* served as sustainable reducing and stabilizing agent for the synthesis of silver and gold nanoparticles. The flavonoids and phenolic content were responsible for the redox activity. Fatal free radicals have been removed in-vitro manner using DPPH model. Antimicrobial activity of nanometals towards two Gram negative, two Gram positive and two fungal stains were established. The catalytic power of silver and gold particles has been proved here for the degradation of methylene blue, rhodamine B and reduction of 4-nitrophenol by  $\text{NaBH}_4$ .

## MATERIALS AND METHODS

All materials used were of analytical grade and silver nitrate ( $\text{AgNO}_3$ ), methylene blue, rhodamine B, 4-nitrophenol and sodium borohydride ( $\text{NaBH}_4$ ) were purchased from Merck India Ltd. Chloroauric acid ( $\text{HAuCl}_4 \cdot 3\text{H}_2\text{O}$ ) was purchased from Sigma Aldrich and used as received without additional purification and all solutions were prepared in Millipore water.

**Preparation of *Jatropha curcas* L Leaf Extract:** *Jatropha curcas* L (*J. curcas*) were taxonomically identified and fresh leaves were collected and washed repeatedly using Millipore water and air dried for two days. 5 g of dried leaves were heated in 100 mL distilled water for 20 minutes at 60°C. It was cooled and filtered through Whatmann No.40 filter paper and kept at 4°C for the preparation of nanoparticles.

Plant-mediated facile synthesis of silver and

gold nanoparticles: In the present nanoparticles synthesis, 90 mL  $\text{AgNO}_3 / \text{HAuCl}_4$  (1 mM) was taken along with 10 mL of leaf extract in a 250mL beaker. The reaction mixtures were exposed to microwave radiation using a house-hold microwave oven (Sharp R-219T (W)) [13]. Formation of silver and gold nanoparticles was identified by visual color change of the medium and was confirmed using UV-vis. spectrophotometer operating in the wavelength range 200-800 nm. Nanoparticles were separated in high-speed centrifuge under refrigeration and the purified samples were used for further analysis.

**Characterization:** UV-vis. spectra were collected on a Shimadzu UV-2450 spectrophotometer. Fourier Transform infrared (FT-IR) spectra were recorded on PerkinElmer Spectrum Two Infrared spectrometer with ATR facility. JEOL JEM-2100 microscope with EDX attachment captured the HR-TEM images. Powder XRD measurements were performed by Bruker AXS D8 Advance X-ray diffractometer. AFM analysis were done using WITec Alpha 300 RA machine in the tapping mode.

### *In-vitro antioxidant assay*

The antioxidant capacities of the synthesized nanoparticles in terms of hydrogen donating ability were estimated using DPPH assay [14]. DPPH is 1, 1- diphenyl-2-picryl hydrazyl, a stable free radical. Different concentrations of antioxidant solutions were mixed with 0.1 mM DPPH solution in DMSO under dark condition and kept it at room temperature for 20 minutes incubation. The absorbance at 517 nm was measured using UV- vis. spectrophotometer. Control experiment was also conducted. Plant extract, synthesized silver/gold nanoparticles were employed in the assessment process using ascorbic acid as the standard of reference. Each analysis was triplicated and the average percentage of DPPH-scavenging was calculated.

$$\text{Inhibition (\%)} = \frac{\text{control} - \text{test}}{\text{control}} \times 100$$

### *Antimicrobial assay*

The in-vitro antimicrobial potential of the microwave generated metal nanoparticles was estimated using the agar well-diffusion method. Two Gram positive (*Bacillus cereus*-MTCC 1305 and *Staphylococcus aureus*-MTCC 96) and two Gram negative (*Escherichia coli*-MTCC 443) and *Pseudomonas aeruginosa*-MTCC 424)) bacterial

stains and two fungal stains (*Aspergillus nidulans*-MTCC 11267 and *Aspergillus flavus*-MTCC 277) originally obtained from Microbial Type Culture Collection, Chandigarh, India were used. Wells of about 6 mm diameter were bored using a well cutter on grown microbes and 50  $\mu$ L of the aqueous extract (0.05 mg/ mL), silver and gold nanoparticles (1 mg/ mL) were poured in to separate wells and were incubated for 24 hours in the case of bacteria and 1 week in the case of fungi and the inhibitory zone in mm was measured. Streptomycin/ griseofulvin (10 mg/ mL) was used as the positive control for antibacterial and antifungal studies and double distilled water constituted the negative control. Measurements were replicated and the mean diameter was calculated which reflected the inhibitory nature of the nanoparticles.

#### Statistical Analysis

All the data were expressed as mean  $\pm$  standard deviation and the results were analysed by one way ANOVA followed by Tukey's Post hoc analysis using Graph pad Prism software. A value of  $p < 0.05$  was considered as statistically significant.

#### Catalytic capacity

Dyes were generally colouring chemicals. Removal of toxic dye stuffs from various industrial effluents was inevitable for the better aquatic life. Catalytic ability of silver and gold nanoparticles (0.02 mg/ mL) was exploited for the removal of

methylene blue and rhodamine B using  $\text{NaBH}_4$  reducing agent. Methylene blue ( $8 \times 10^{-5} \text{M}$ ) or rhodamine B ( $5 \times 10^{-5} \text{M}$ ) were mixed with  $\text{NaBH}_4$  (0.06 M) and fixed amount of the nanocatalysts (0.02 mg/ mL). Control experiments without nanocatalysts were also executed. The periodic monitoring of the degradation reaction was done by UV-vis. spectral observations of the reaction mixture at regular intervals. Kinetic parameters of the reactions were also found out.

Hydrogenation of 4-nitrophenol ( $8 \times 10^{-5} \text{M}$ ) to 4-aminophenol by  $\text{NaBH}_4$  (0.06 M) was also studied in the presence of the nanocatalysts (0.02 mg/ mL). Hydrogenation of 4-nitrophenol when no catalysts present were also accomplished. Progress of the reaction was followed by depletion in absorbance at 400 nm in UV-vis. absorption spectra and kinetics was investigated.

## RESULTS AND DISCUSSION

#### Particle characterization

Developments of silver/ gold nanoparticles were indicated by the onset of brown (b) and ruby red colour (c) to the reaction medium (Fig. 1) containing the plant extract which was colourless (a). Silver and gold nanoparticles were abbreviated respectively as AgNP-J.curcas and AuNP-J.curcas.

#### UV-vis. spectroscopy

UV-vis. absorption spectra of AgNP-J.curcas (Fig. 1d) and AuNP-J.curcas (Fig. 1e) exhibit

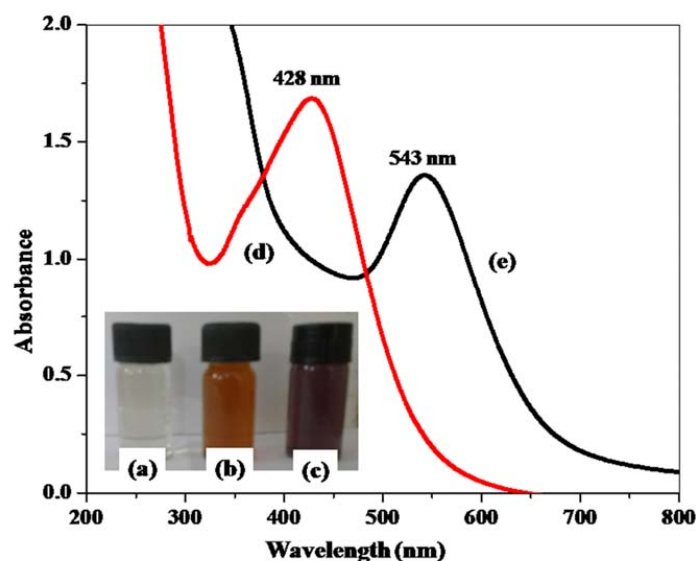


Fig. 1. Photograph of (a) J.curcas leaf extract, (b) AgNP-J.curcas, (c) AuNP-J. curcas, (d) UV-vis. absorption spectra of AuNP-J.curcas and (e) AgNP-J.curcas

characteristic optical property, surface plasmon resonance, at 428 nm and 543 nm respectively. The sharp and symmetric SPR peaks reflected spherical shape of nanometals which was further set out in TEM analyses [15].

#### FT-IR spectroscopy

Phytochemicals present in *J. curcas* for reduction and capping of metal nanoparticles were identified by FT-IR analysis. *J. curcas* produced peaks at 3261, 1605, 1403, 1304 and 1014  $\text{cm}^{-1}$  (Fig. 2(a)). Intense band at 3261  $\text{cm}^{-1}$  was due to O-H stretching of alcohols and phenols, small peak just above 3000  $\text{cm}^{-1}$  was by aromatic C-H stretching, strong and sharp band at 1605  $\text{cm}^{-1}$  may be due to C=C stretching in aromatics or amide group. Band at 1403  $\text{cm}^{-1}$  was due to C-O-H in plane bending of hydroxyl group. 1304  $\text{cm}^{-1}$

was coming from C-O stretching mode [16] and weak band at 1014  $\text{cm}^{-1}$  was by C-O-C stretching [17]. All vibrational peaks clearly indicated the presence of phenolic compounds. The IR bands from AgNP-*J. curcas* and AuNP-*J. curcas* were 3360, 1605, 1321  $\text{cm}^{-1}$  (Fig. 2(b)) and 3252, 1606, 1403, 1303, 1047  $\text{cm}^{-1}$  (Fig. 2(c)) respectively. Relatively fair peaks at identical positions manifested the capping action by the biomolecules. Silver nanoparticles reported from latex and seed extract of *J. curcas* strongly supported the involvement of amide functionality in reduction and stabilization processes (9,10).

#### XRD

The crystalline character of microwave synthesized nanometals was unveiled by XRD analysis (Fig. 3). The crystallographic analysis

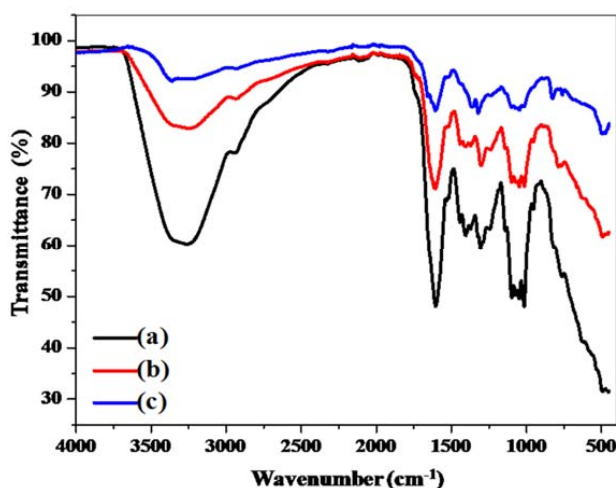


Fig. 2. FT-IR spectra of (a) *J. curcas* leaf extract, (b) AgNP-*J. curcas* and (c) AuNP-*J. curcas*

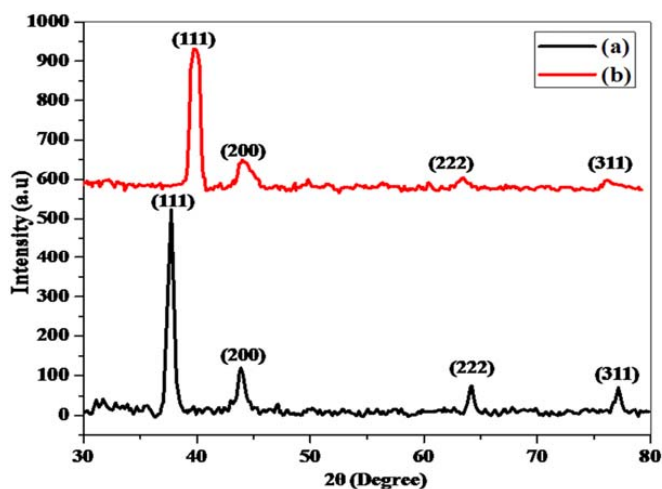


Fig. 3. XRD pattern of (a) AgNP-*J. curcas* and (b) AuNP-*J. curcas*

for (a) AgNP-J.curcas gave peaks at scan angles 37.72°, 43.87°, 64.19°, 77.17° and (b) AuNP-J. curcas produce peaks at 37.87°, 44.08°, 64.04° and 77.54°. They were indexed to reflections originated from (111), (200), (220) and (311) faces of FCC nanosilver and nanogold. Sharp and intense peak from (111) plane denoted the preferred orientation of the crystals.

The average crystallite size calculated using Debye-Scherrer formula (1) for (111) plane of AgNP-J.curcas and AuNP-J.curcas were 19.00 nm and 7.63 nm. The average particle size calculated by XRD data was in agreement with TEM data in

the case of AgNP-J.curcas, but found smaller in the case of AuNP-J.curcas.

$$D = 0.9\lambda / \beta \cos\theta$$

Where, D- Particle size,  $\beta$ - FWHM,  $\theta$ - Angle of diffraction, Wavelength ( $\lambda$ ) for x-ray = 0.1541 nm

#### TEM-EDX

The morphologies of microwave synthesized silver (Fig. 4) and gold (Fig. 5) nanoparticles were cleared from TEM images at different magnifications. Morphological information collected from TEM analysis showed spherical

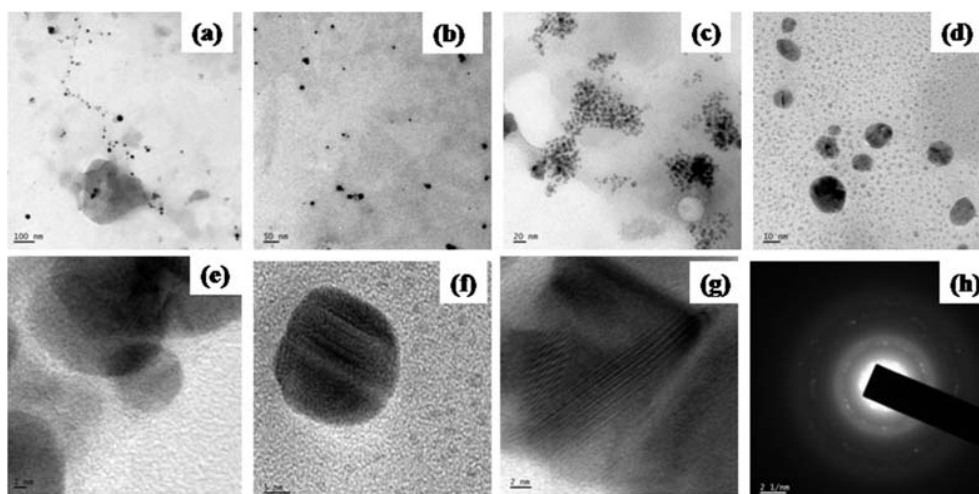


Fig. 4. TEM photographs of AgNP-J.curcas, (a-f) images at different magnifications, (g) HR-TEM image showing lattice fringes and (h) SAED pattern

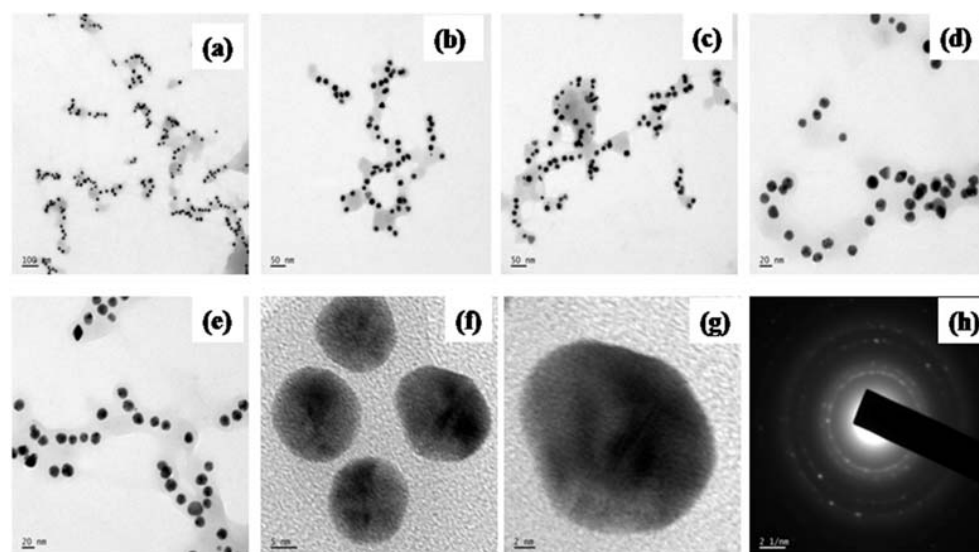


Fig. 5. TEM photographs of AuNP-J.curcas, (a-g) images at different magnifications and (h) SAED pattern

geometry for silver nanoparticles (d-f). Lattice fringes were clearly visible in HR-TEM images (g) and d-spacing was calculated as  $2.36\text{\AA}$  (16). SAED pattern showed bright circular spots supporting the crystallinity of AgNP-J.curcas.

AuNP-J.curcas was roughly spherical and SAED pattern contained bright spots arising from Bragg reflections from various crystallites of FCC nanocrystal, proving the crystalline nature [18]. The capping actions provided by biomolecules from J.curcas were clearly visible from microscopic images of nanoparticles at different magnifications [19].

Energy Dispersive X-ray spectroscopy, Fig. 6(a) and 6(b) confirmed the attendance of metallic silver and gold. Presence of carbon and oxygen that came from biomolecules were also seen in the Fig. 6(b) (20). Particle size histogram (Fig. 6(c,d)) settled the distribution of nanoparticles and the average diameter of silver and gold nanoparticles were calculated using Image J software as  $20.42\pm 12.2$  and  $17.12\pm 2.9$  nm respectively. We were able to synthesize small sized nanoparticles and the average size of silver nanoparticles found larger than that of gold.

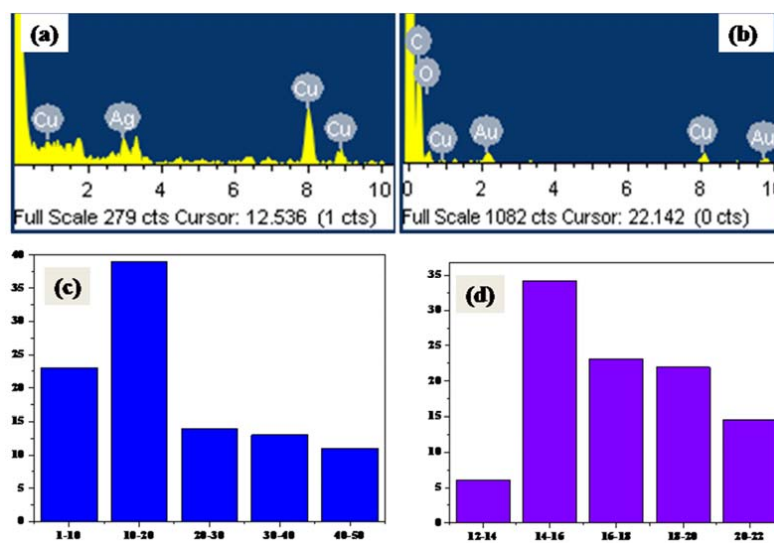


Fig. 6. EDX spectra of (a) AgNP-J.curcas and (b) AuNP-J.curcas, particle size distribution of (c) AgNP-J.curcas and (d) AuNP-J.curcas

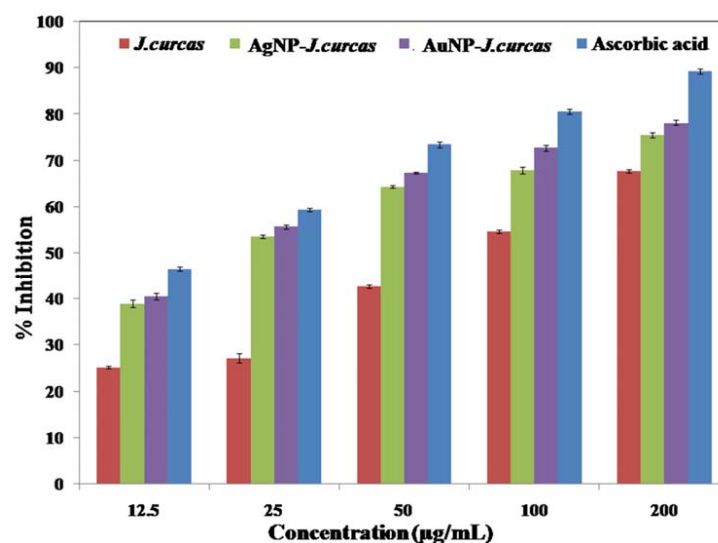


Fig. 7. DPPH scavenging activity of J.curcas, AgNP-J.curcas and AuNP-J.curcas were compared with ascorbic acid standard. Values are Mean±SD (n=3)

**AFM**

Three and two dimensional images of nanoparticles were obtained from surface scanning in AFM analysis showed an uneven distribution of particles and had tendency to agglomerate on deposition [21]. The average roughness of AgNP-J. curcas and AuNP-J. curcas were found to be 3.33 nm 4.78 nm.

**Antioxidant power-DPPH method**

Diseases caused through oxidative stress were controlled by antioxidant materials. Facile synthesized silver and gold nanoparticles exhibited excellent free radical capturing power (Fig. 7). IC<sub>50</sub> values obtained from GraphPad Prism software for J. curcas, AgNP-J. curcas and AuNP-J. curcas are 75.87±1.36, 19.37±0.63 and 16.59±0.29 µg/ mL respectively. IC<sub>50</sub> value represented the concentration of antioxidant corresponding to 50% inhibition [22] non-toxic and environmentally benign synthetic design for the fabrication of metal nanoparticles has led to the use of essential oil present in plant parts as the bioreductant. In this report, silver particles at nanoscale have been synthesized using essential oil present in the leaves of Coleus aromaticus at physiological pH and at 373 K. UV-vis spectra of the colloid display strong plasmon bands centred around 396-411 nm, characteristic of silver nanoparticles. Comparative studies of the FTIR spectra of essential oil and silver nanoparticles

reveal the involvement of terpenes and their phenolic derivatives in reduction and subsequent stabilization. TEM micrographs and XRD pattern show the formation of 26 and 28 nm sized face centred cubic structured crystalline nanospheroids with intermittent formation of nanorods. The phytosynthesized silver nanoparticles are found to be effective in degrading hazardous organic pollutants including methyl orange, methylene blue, eosin yellowish and para nitro phenol within a span of a few minutes. Dose dependant antibacterial activity of the biogenic nanosilver against pathogenic Gramme-negative Escherichia coli (ATCC 25922. The radical terminating power showed direct correlation with the amount of substance used. The noble metal nanoparticles showed pronounced antioxidant potential than the plant extract and was comparable to that of reference, ascorbic acid (IC<sub>50</sub>=14.67±0.30 µg/ mL). Phenols (flavonoids and tannins) present in the aqueous leaf extract of J. curcas [23,24] were responsible for the antioxidant characteristics of colloidal nanoparticles derived from it. Reports showed that ethanol extract of leaves of J. curcas had flavanones apigenin, orientin, vitexin and rhoifolin [8,25] 2-diphenyl-1-picrylhydrazyl. J. curcas reduced metal nanoparticles offer an effective natural antioxidant source which can protect cells and prevent lifestyle-related illnesses [26]. The statistical analysis by one way ANOVA proved the statistical significance of the data and the post-hoc

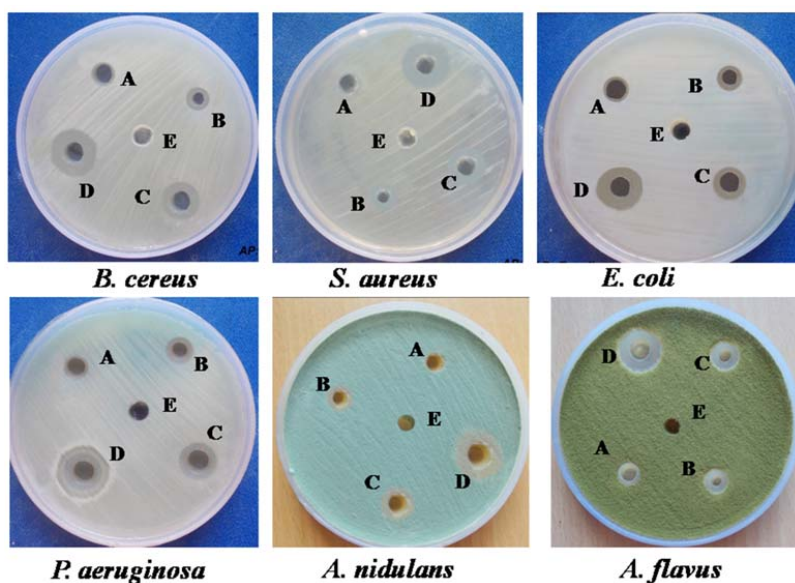


Fig. 8. Photographs of petriplates used in agar-well diffusion method. A =J. curcas leaf extract, B= AuNP-J. curcas, C=AgNP-J. curcas, D= positive control and E=negative control

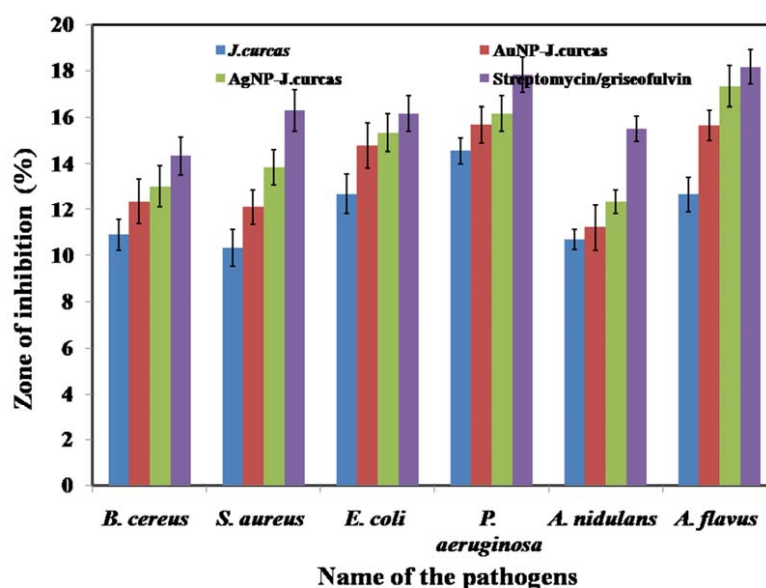


Fig. 9. Inhibition zone (%) produced by J.curcas leaf extract, AgNP-J.curcas and AuNP-J.curcas towards various microorganisms. Values are Mean $\pm$ SD (n=6)

analysis by Tukey's test showed the mean values increases in the order J.curcas < AgNP-J.curcas < AuNP-J.curcas and thus the antioxidant power follows the same order.

#### Antimicrobial study

The agar well diffusion method displayed broad spectrum of activity against the stains of microorganisms tested (Fig. 8). AuNP-J.curcas and AgNP-J.curcas have shown zone of inhibition larger than the leaf extract J.curcas (Fig. 9).

Antimicrobial power of nanometals exceeded that of J.curcas. Total phenolics present in the leaf extract substantially built a barrier against the invading organisms [27]. Noble nanoparticles have a preferred affinity towards sulphur and phosphorous protein moieties in bacterial cell membranes [28] which lead to cell viability. Bacterial death caused through rupturing cell wall by nanoparticles lead to inhibition zone [29]. In Gram positive bacteria, the protecting peptidoglycan layer resisted the action of nanometals and resulting in lower zone of inhibition compared to Gram negative ones [30]. An exceptionally higher inhibition value was shown by Gram negative bacteria *P. aeruginosa* [27].

#### Catalytic power of metal nanoparticles

The catalytic power of nanometals can be utilized in environment cleanup process mainly

for removal of dyes from industrial waste water. In aqueous medium methylene blue and rhodamine B have absorption maxima at 664 and 553 nm respectively. In the absence of catalyst, the toxic dyes were feebly degraded solely by NaBH<sub>4</sub> (Fig. 10(a) and (b)).

An important starting chemical of most of the pesticides and organic dyes, namely 4-nitrophenol has been listed as a toxic pollutant by Environment Protection Agency of US. 4-nitrophenol has  $\lambda_{max}$  317 nm in aqueous phase which shifted to 400 nm when NaBH<sub>4</sub> was added followed by intensification of its yellow color. This was because of 4-nitrophenolate ion formed in alkaline medium and was highly stabilized by resonance [31]. Reduction of 4-nitrophenol to 4-aminophenol was seldom possible by NaBH<sub>4</sub> alone (Fig.10 (c)). Even after 10minutes no peak corresponding to the product 4-aminophenol was observed. The potential energy barrier between electron donor H<sub>3</sub>BO<sub>3</sub>/NaBH<sub>4</sub><sup>-</sup> and acceptor 4-NP/4-AP is large enough to prevent the reaction to proceed [32] green method is described for the synthesis of Gold (Au).

Adsorptive removal of dyes and reduction of 4-nitrophenol on silver catalytic surface by NaBH<sub>4</sub> were shown in Fig. 11. Methylene blue degradation on AgNP-J.curcas ended within 12minutes (a). Rhodamine B degraded within a time span of 7minutes on the surface of silver nanocatalysts

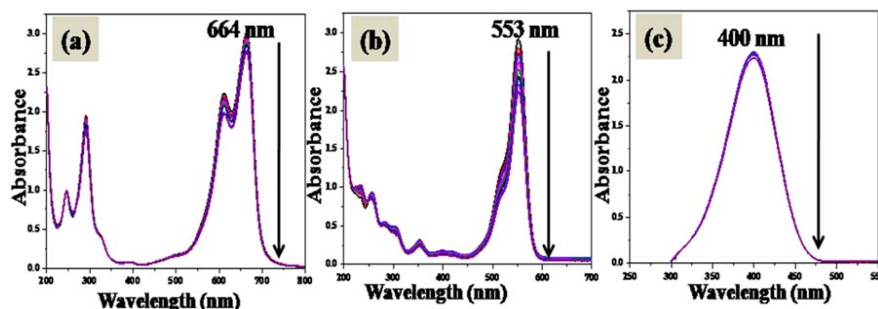


Fig. 10. Reduction of (a) methylene blue, (b) rhodamine B and (c) 4-nitrophenol by  $\text{NaBH}_4$

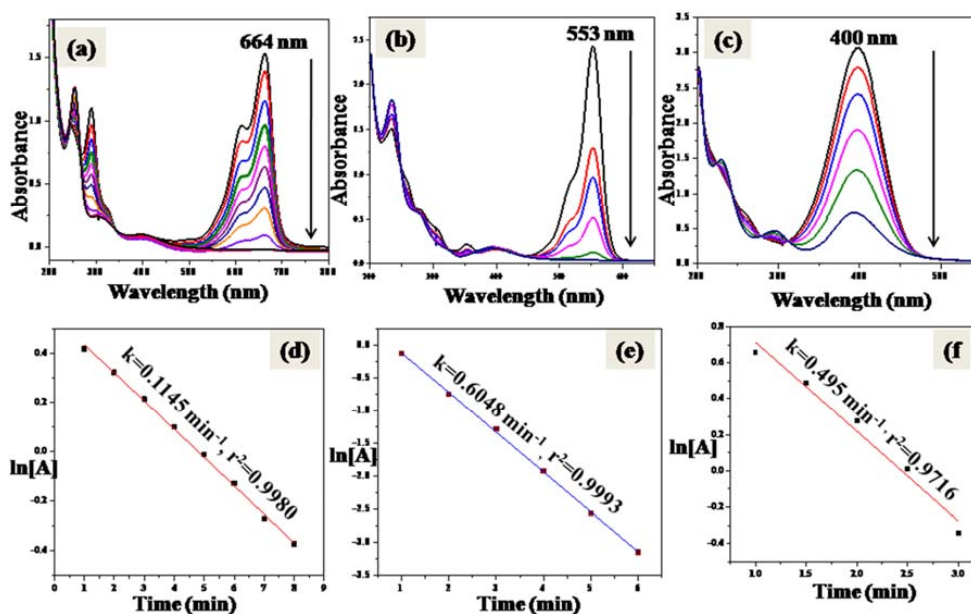


Fig. 11. Degradation of (a) methylene blue, (b) rhodamine B and (c) reduction of 4-nitrophenol catalyzed by AgNP-J. curcas. (d-f) respective kinetic plots ( $\ln[A]$  verses time)

(b). In the case of 4-nitrophenol, when 0.5 mL AgNP-J. curcas was added to the reaction mixture, dramatically the reduction reaction was accelerated and ended in 8 minutes (c).

The inadequate degradation of methylene blue and rhodamine B by  $\text{NaBH}_4$  was overwhelmed within 10 minutes by the nanocatalyst, AuNP-J. curcas (Fig. 12). 10 minutes was needed for the reduction of 4-nitrophenol.

Since the high surface area provided by nanocatalysts was ample enough, the dye and  $\text{NaBH}_4$  molecules get adsorbed at the surface of the nanocatalysts and the electrons were transferred from the donor  $\text{BH}_4^-$  to the acceptor organic dyes [11]. The mechanism was through an electron relay process and the catalysts acted as

redox centre [33]. Rate constant determination proved pseudo first order kinetics with respect to dye concentration, since the amount of  $\text{NaBH}_4$  used is too high. The rate equation is:

$$k = \frac{1}{t} \ln[A] / [A]_0$$

where  $k$  is the pseudo-first order rate constant,  $[A_0]$  and  $[A]$  are the concentrations of the reactant at time zero and  $t$ .

In the case of reduction of 4-nitrophenol, the electron transfer reaction between donor and acceptor happened [22] non-toxic and environmentally benign synthetic design for the fabrication of metal nanoparticles has led to the use of essential oil present in plant parts as

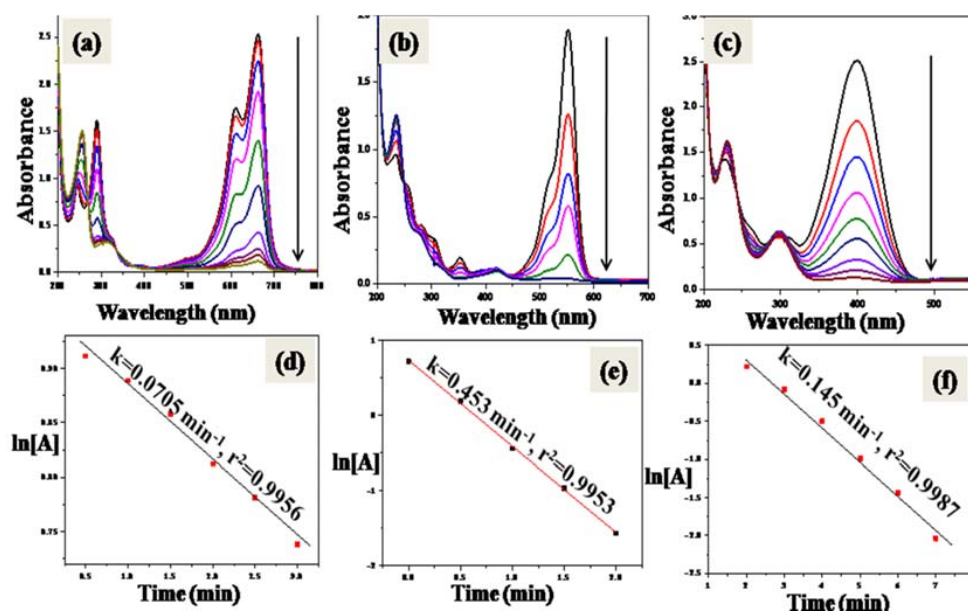


Fig. 12. Degradation of (a) methylene blue, (b) rhodamine B and (c) reduction of 4-nitrophenol catalyzed by AuNP-J.curcas. (d-f) linear plot of  $\ln[A]$  versus time for the above mentioned reactions (c)

the bioreductant. In this report, silver particles at nanoscale have been synthesized using essential oil present in the leaves of *Coleus aromaticus* at physiological pH and at 373 K. UV-vis spectra of the colloid display strong plasmon bands centred around 396-411 nm, characteristic of silver nanoparticles. Comparative studies of the FTIR spectra of essential oil and silver nanoparticles reveal the involvement of terpenes and their phenolic derivatives in reduction and subsequent stabilization. TEM micrographs and XRD pattern show the formation of 26 and 28 nm sized face centred cubic structured crystalline nanospheroids with intermittent formation of nanorods. The phytosynthesized silver nanoparticles are found to be effective in degrading hazardous organic pollutants including methyl orange, methylene blue, eosin yellowish and para nitro phenol within a span of a few minutes. Dose dependant antibacterial activity of the biogenic nanosilver against pathogenic Gramme-negative *Escherichia coli* (ATCC 25922 along with transfer of surface hydrogens by adsorbing on the surface of the nanocatalysts by Langmuir-Hinshelwood model [34]. The sudden depletion of  $\lambda_{\text{max}}$  at 400 nm verified the reactant disappearance. The new peak at 298nm confirmed the product formation, the amine. Linear plot between  $\ln[A]$  and reaction time set up the calculation of rate constants from slopes. The graph confirmed the inverse correlation between concentration of 4-NP and reaction time.

The amount of reducing agent used is 750-fold higher as compared to reactant concentration,  $[\text{NaBH}_4]$  virtually unaltered and taken as constant. Thus the reaction followed pseudo-first order kinetics with respect to reactant concentration.

## CONCLUSIONS

All the parts of *J.curcas* were useful to humanity in one way or other. The aqueous leaf extract functioned as reducing and anti agglomerating agent in the present microwave assisted synthesis. Silver and gold nanoparticles proved their biological properties as antioxidants and antimicrobials and can be beneficially exploited in medical field. The catalytic properties shown by nanometals may be implemented in purification of effluents from various industries. The catalytic power of silver and gold nanoparticles can be utilized in the reduction of 4-nitrophenol.

## ACKNOWLEDGEMENTS

The authors gratefully acknowledged the financial assistance to Sijo Francis from University Grants Commission (under Faculty Development Programme), Government of India.

## CONFLICT OF INTEREST

The author declares that there is no conflict of interests regarding the publication of this manuscript.

## REFERENCES

- Raut RW, Mendhulkar VD, Kashid SB. Photosensitized synthesis of silver nanoparticles using *Withania somnifera* leaf powder and silver nitrate. *J Photochem Photobiol B Biol.* 2014;132(February 2016):45–55.
- Nadagouda MN, Varma RS. Green synthesis of silver and palladium nanoparticles at room temperature using coffee and tea extract. *Green Chem.* 2008;10(8):859.
- Jagtap UB, Bapat VA. Green synthesis of silver nanoparticles using *Artocarpus heterophyllus* Lam. seed extract and its antibacterial activity. *Ind Crops Prod.* 2013;46:132–137.
- Francis S, Joseph S, Koshy EP, Mathew B. Synthesis and characterization of multifunctional gold and silver nanoparticles using leaf extract of: *Naregamia alata* and their applications in the catalysis and control of mastitis. *New J Chem.* 2017;41(23).
- Joseph S, Mathew B. Microwave Assisted Biosynthesis of Silver Nanoparticles Using the Rhizome Extract of *Alpinia galanga* and Evaluation of Their Catalytic and Antimicrobial Activities. *J Nanoparticles.* 2014;2014:9.
- Francis S, Joseph S, Koshy EP, Mathew B. Green synthesis and characterization of gold and silver nanoparticles using *Mussaenda glabrata* leaf extract and their environmental applications to dye degradation. *Environ Sci Pollut Res.* 2017;24(21):17347–17357.
- Francis S, Joseph S, Koshy EP, Mathew B. Microwave assisted green synthesis of silver nanoparticles using leaf extract of *elephantopus scaber* and its environmental and biological applications. *Artif Cells, Nanomedicine, Biotechnol.* 2017;(0):1–10.
- Kumar A, Sharma S. An evaluation of multipurpose oil seed crop for industrial uses (*Jatropha curcas* L.): A review. *Ind Crops Prod.* 2008;28(1):1–10.
- Bar H, Bhui DK, Sahoo GP, Sarkar P, Pyne S, Misra A. Green synthesis of silver nanoparticles using seed extract of *Jatropha curcas*. *Colloids Surfaces A Physicochem Eng Asp.* 2009;348(1–3):212–216.
- Bar H, Bhui DK, Sahoo GP, Sarkar P, De SP, Misra A. Green synthesis of silver nanoparticles using latex of *Jatropha curcas*. *Colloids Surfaces A Physicochem Eng Asp.* 2009;339(1–3):134–139.
- Sheikh Mohamed M, Baliyan A, Veerananayanan S, Cheruvathoor Poulose A, Nagaoka Y, Minegishi H, et al. Non-Destructive Harvesting of Biogenic Gold Nanoparticles from *Jatropha curcas* Seed Meal and Shell Extracts and their Application as Bio-Diagnostic Photothermal Ablaters-Lending Shine to the Biodiesel Byproducts. *Nanomater Environ.* 2013;1(August):3–17.
- Chauhan N, Tyagi AK, Kumar P, Malik A. Antibacterial potential of *Jatropha curcas* synthesized silver nanoparticles against food borne pathogens. *Front Microbiol.* 2016;7(NOV):1–13.
- Joseph S, Mathew B. Microwave-assisted facile synthesis of silver nanoparticles in aqueous medium and investigation of their catalytic and antibacterial activities. *J Mol Liq.* 2014;197:346–352.
- Choi CW, Kim SC, Hwang SS, Choi BK, Ahn HJ, Lee MY, et al. Antioxidant activity and free radical scavenging capacity between Korean medicinal plants and flavonoids by assay-guided comparison. *Plant Sci.* 2002;163(6):1161–1168.
- Chavada VD, Bhatt NM, Sanyal M, Shrivastav PS. Surface plasmon resonance based selective and sensitive colorimetric determination of azithromycin using unmodified silver nanoparticles in pharmaceuticals and human plasma. *Spectrochim Acta - Part A Mol Biomol Spectrosc.* 2017;170:97–103.
- Philip D, Unni C. Extracellular biosynthesis of gold and silver nanoparticles using *Krishna tulsi* (*Ocimum sanctum*) leaf. *Phys E Low-Dimensional Syst Nanostructures.* 2011;43(7):1318–1322.
- Sathishkumar G, Jha PK, Vignesh V, Rajkuberan C, Jeyaraj M, Selvakumar M, et al. Cannonball fruit (*Couroupita guianensis*, Aubl.) extract mediated synthesis of gold nanoparticles and evaluation of its antioxidant activity. *J Mol Liq.* 2016;215:229–236.
- Sujitha M V., Kannan S. Green synthesis of gold nanoparticles using Citrus fruits (*Citrus limon*, *Citrus reticulata* and *Citrus sinensis*) aqueous extract and its characterization. *Spectrochim Acta - Part A Mol Biomol Spectrosc.* 2013;102:15–23.
- Velusamy P, Das J, Pachaiappan R, Vaseeharan B, Pandian K. Greener approach for synthesis of antibacterial silver nanoparticles using aqueous solution of neem gum (*Azadirachta indica* L.). *Ind Crops Prod.* 2015;66(1):103–109.
- Kotakadi VS, Gaddam SA, Subba Rao Y, Prasad TNV K V, Varada Reddy A, Sai Gopal DVR. Biofabrication of silver nanoparticles using *Andrographis paniculata*. *Eur J Med Chem.* 2014;73:135–140.
- Christensen L, Vivekanandhan S, Misra M, Mohanty AK. Biosynthesis of silver nanoparticles using *Murraya koenigii* (curry leaf): An investigation on the effect of broth concentration in reduction mechanism and particle size. *Adv Mater Lett.* 2011;2(6):429–434.
- Vilas V, Philip D, Mathew J. Essential oil mediated synthesis of silver nanocrystals for environmental, anti-microbial and antioxidant applications. *Mater Sci Eng C.* 2016;61:429–436.
- Prasad DMR, Izam A, Khan MR. *Jatropha curcas*: Plant of medical benefits. *J Med Plants Res.* 2012;6(14):2691–2699.
- Uche F, Aprioku J. The Phytochemical Constituents, Analgesic and Anti-inflammatory effects of methanol extract of *Jatropha curcas* leaves in Mice and Wister albino rats. *J Appl Sci Environ Manag.* 2010;12(4).
- Huang Q, Guo Y, Fu R, Peng T, Zhang Y, Chen F. Antioxidant activity of flavonoids from leaves of *Jatropha curcas*. *ScienceAsia.* 2014;40(3):193–197.
- Kalantari K, Afifi ABM, Bayat S, Shameli K, Yousefi S, Mokhtar N, et al. Heterogeneous catalysis in 4-nitrophenol degradation and antioxidant activities of silver nanoparticles embedded in Tapioca starch. *Arab J Chem.* 2017.
- Oskoueian E, Abdullah N, Ahmad S, Saad WZ, Omar AR, Ho YW. Bioactive compounds and biological activities of *Jatropha curcas* L. kernel meal extract. *Int J Mol Sci.* 2011;12(9):5955–5970.
- Sulaiman GM, Mohammed WH, Marzoog TR, Al-Amiery AAA, Kadhum AAH, Mohamad AB. Green synthesis, antimicrobial and cytotoxic effects of silver nanoparticles using *Eucalyptus chapmaniana* leaves extract. *Asian Pac J Trop Biomed.* 2013;3(1):58–63.
- Perugu S, Nagati V, Bhanoori M. Green synthesis of silver nanoparticles using leaf extract of medicinally potent plant *Saraca indica* : a novel study. *Appl Nanosci.* 2015;6:747–753.
- Mariselvam R, Ranjitsingh AJA, Usha Raja Nanthini A,

- Kalirajan K, Padmalatha C, Mosae Selvakumar P. Green synthesis of silver nanoparticles from the extract of the inflorescence of *Cocos nucifera* (Family: Arecaceae) for enhanced antibacterial activity. *Spectrochim Acta - Part A Mol Biomol Spectrosc.* 2014;129:537–541.
31. Dash SS, Bag BG, Hota P. Lantana camara Linn leaf extract mediated green synthesis of gold nanoparticles and study of its catalytic activity. *Appl Nanosci.* 2014;3:343–350.
32. Gangula A, Podila R, M R, Karanam L, Janardhana C, Rao AM. Catalytic reduction of 4-nitrophenol using Biogenic Gold and Silver Nanoparticles Derived from *Breynia rhamnoides*. *Langmuir.* 2011;27(24):15268–15274.
33. Edison TJI, Sethuraman MG. Instant green synthesis of silver nanoparticles using *Terminalia chebula* fruit extract and evaluation of their catalytic activity on reduction of methylene blue. *Process Biochem.* 2012;47(9):1351–1357.
34. Ajitha B, Reddy YAK, Reddy PS, Suneetha Y, Jeon H-J, Ahn CW. Instant biosynthesis of silver nanoparticles using *Lawsonia inermis* leaf extract: Innate catalytic, antimicrobial and antioxidant activities. *J Mol Liq.* 2016;219:474–481.